HHS Public Access

Author manuscript

*Nat Neurosci*. Author manuscript; available in PMC 2019 January 23.

Published in final edited form as:

*Nat Neurosci*. 2018 August ; 21(8): 1038–1048. doi:10.1038/s41593-018-0194-1.

# Pathogenic tau-induced piRNA depletion promotes neuronal death through transposable element dysregulation in neurodegenerative tauopathies

**Wenyan Sun, Ph.D.**[1,2,4], **Hanie Samimi**[3], **Maria Gamez**[1,4], **Habil Zare, Ph.D.**[4], and **Bess Frost, Ph.D.**[1,4,5,*]

[1]Barshop Institute for Longevity and Aging Studies, San Antonio, Texas 78245, USA

[2]Department of Nutrition and Food Security, School of Public Health, Xi'an Jiaotong University, Xi'an, 710061, China

[3]Department of Computer Science, Texas State University, San Marcos, Texas 78666, USA

[4]Department of Cell Systems and Anatomy, University of Texas Health San Antonio, San Antonio, Texas 78229, USA

[5]Glenn Biggs Institute for Alzheimer's & Neurodegenerative Diseases, San Antonio, Texas 78229, USA

## Abstract

Transposable elements, known colloquially as "jumping genes," constitute approximately 45% of the human genome. Cells utilize epigenetic defenses to limit transposable element jumping, including formation of silencing heterochromatin and generation of piwi-interacting RNAs (piRNAs), small RNAs that facilitate clearance of transposable element transcripts. Here we identify transposable element dysregulation as a key mediator of neuronal death in tauopathies, a group of neurodegenerative disorders that are pathologically characterized by deposits of tau protein in the brain. Mechanistically, we find that heterochromatin decondensation and reduction of piwi/piRNAs drive transposable element dysregulation in tauopathy. We further report a significant increase in transcripts of the endogenous retrovirus class of transposable elements in human Alzheimer's disease and progressive supranuclear palsy, suggesting that transposable element dysregulation is conserved in human tauopathy. Taken together, our data identify heterochromatin decondensation, piwi/piRNA depletion and consequent transposable element



*Correspondence should be addressed to B.F. (bfrost@uthscsa.edu).

**Author Contributions.** WS and BF conceived the study and analyzed the data. WS and MG performed experiments. HS and HZ performed RNA-seq analysis. WS, HZ, and BF contributed to writing the manuscript. All authors reviewed the manuscript.

**Accession codes.** Full access to fastq files that include Drosophila transposable element and piRNA is provided through the Gene Expression Omnibus (GEO) database (GSE115606).

**Competing Financial Interests Statement.** The authors declare no competing financial interests.

**Code availability.** Custom codes that were created for cleaning and analyzing sequencing data are available in Supplementary Software and can also be accessed at https://bitbucket.org/habilzare/alzheimer.

**Data availability.** Raw counts from RNA sequencing are provided as Supplementary Tables. The data that support the findings of this study are available from the corresponding author upon reasonable request.

dysregulation as a novel, pharmacologically targetable, mechanistic driver of neurodegeneration in tauopathy.

Transposable elements are categorized as Class I, the retrotransposons, or Class II, the DNA transposons. Retrotransposons are structurally akin to retroviruses in that they require an RNA intermediate to mobilize. Unlike retroviruses, however, retrotransposons lack the ability to move between individuals. DNA transposons, which mobilize via a “cut and paste” mechanism, are thought to have lost the ability to mobilize in the human genome due to imprecise excision and insertion[1]. Organisms ranging from yeast to humans have developed cellular control mechanisms to limit potentially deleterious transposable element activation. Many transposable elements are embedded within highly condensed constitutive heterochromatin, and are thus epigenetically silenced[2]. In addition, transposable element transcripts are the targets of a well-conserved pathway involving piRNAs, small regulatory RNAs that bind to transposable element transcripts and mediate their degradation[3].

The “transposon theory of aging” posits that transposable elements become deleteriously activated as cellular defense and surveillance mechanisms break down with age[4,5]. While transposable element activation has also been implicated in cancer[6], and TDP-43 mediated neurodegeneration[7–9], the extent to which transposable elements are involved in human disorders and drive disease pathogenesis is currently unknown. We have previously identified tau-induced decondensation of constitutive heterochromatin as a key event that mediates neuronal death in tauopathy[10]. We hypothesized that tau-mediated decondensation of constitutive heterochromatin causes epigenetic de-silencing of transposable elements in the context of Alzheimer’s disease and associated tauopathies.

Beginning with a simple model of tauopathy in *Drosophila melanogaster*[11], we report significantly altered levels of transposable element transcripts as a consequence of human tau expression in the adult brain. We identify heterochromatin decondensation and depletion of piwi/piRNAs as major mechanistic links between pathogenic tau and loss of transposable element control, and demonstrate that pathogenic tau causes active transposable element mobilization in neurons. Dietary restriction and 3TC (lamivudine), a nucleoside analog inhibitor of reverse transcriptase that is FDA-approved for the treatment of HIV and Hepatitis B, suppress tau-induced transposable element dysregulation and tau-induced neurotoxicity. Using a systematic, unbiased approach, we identify transposable elements that are differentially expressed in postmortem human brain tissue from patients with Alzheimer’s disease and progressive supranuclear palsy, a “primary” tauopathy, and find that the endogenous retrovirus class of transposable elements is increased in the context of human tauopathy. Taken together, our studies identify heterochromatin decondensation and depletion of piwi and piRNAs as key mechanisms driving transposable element dysregulation and subsequent neuronal death in tau-mediated neurodegeneration. In addition, we show that that suppression of transposable element mobilization and resulting neurodegeneration can be achieved by environmental and pharmacological intervention.

## RESULTS

### *Drosophila* models of human tauopathy have altered levels of transposable element transcripts

*Drosophila melanogaster* provides a genetically tractable platform that can be used to identify cellular mechanisms implicated in disease states and to determine if they are causal for the disease process. To investigate a potential role for transposable element dysregulation as a consequence of pathogenic tau, we began with a *Drosophila* model of tauopathy[11] involving neuron-specific expression of tau$^{R406W}$, a mutant form of human tau that is associated with autosomal dominant tauopathy[12]. *Drosophila* models of human tauopathy have progressive, age-associated neuronal death, a shortened lifespan, and decreased locomotor activity[10,11]. In addition, neuronal phenotypes of tau transgenic *Drosophila* mimic features of human Alzheimer's disease and associated tauopathies, including but not limited to aberrant tau phosphorylation[13], oxidative stress[14], DNA damage[15,16], decondensation of constitutive heterochromatin[10], synaptic dysfunction[17] and activation of the cell cycle in post-mitotic neurons[18].

We performed 100 bp, paired-end sequencing of RNA isolated from control and tau$^{R406W}$ transgenic *Drosophila* heads at day 10 of adulthood, an age at which neuronal death and locomotor deficits are detectable in tau$^{R406W}$ transgenic flies, but prior to the age at which survival is at exponential decline[16]. We identified 50 transposable elements that are significantly increased at the transcript level in tau transgenic *Drosophila* compared to controls, and 60 transposable elements that are significantly decreased (Fig. 1a, unscaled heatmaps are provided in Supplementary Fig. 1, full genotypes are provided in Supplementary Table 1, raw counts are provided in Supplementary Table 2). For several subgroups of transposable elements, we found that multiple members of the same subgroup, such as *copia*, *HeT-A*, and *Quasimodo*, are increased in tau$^{R406W}$ transgenic *Drosophila*, while members of other subgroups, such as *Burdock* and *Blood*, are decreased in tau$^{R406W}$ transgenic *Drosophila.* These data suggest that aberrant expression of transposable elements in tauopathy is a regulated, rather than stochastic, process. The most abundant class of differentially expressed elements in tauopathy are Class I long terminal repeat (LTR) retrotransposons, despite the fact that the majority of transposable elements in *Drosophila* are classified as Class II DNA transposons (Fig. 1b).

The complexity and repetitive nature of transposable elements presents challenges to RNA-seq analysis, which is associated with a greater frequency of false positives and negatives compared to analysis of canonical messenger RNAs. As secondary validation of our RNA-seq analyses, we prepared a custom NanoString codeset consisting of a panel of probes recognizing transposable elements that were identified as differentially expressed in tau transgenic *Drosophila* based on RNA-seq (Supplementary Table 3). NanoString technology combines transcript-specific color-coded barcodes with fluorescent imaging to sensitively quantify transcript levels[19]. When possible, we created "generic" NanoString probes to recognize the differentially expressed transposable elements within a transposable element subgroup (Supplementary Table 4). While a calculation of the fold-change estimate for each element generated by RNA-seq versus the fold-change for NanoString (Supplementary Fig.

1b) suggests a moderate to strong relationship between RNA-seq and NanoString, not all transposable elements that were called as differentially expressed in tau transgenic *Drosophila* based on RNA-seq reach statistical significance based on NanoString analysis. 14 of 25 probes were confirmed by NanoString as significantly increased (Fig. 1c), while 6 of 22 probes were confirmed as significantly decreased in heads of $tau^{R406W}$ transgenic *Drosophila* (Fig. 1d). These analyses also revealed that the transposable elements transcripts that are increased in response to pathogenic tau generally have a greater magnitude of change than transposable element transcripts that are decreased in response to pathogenic tau.

We hypothesized that aberrant transposable element expression is relevant to the larger group of tauopathies, including Alzheimer's disease, that are pathologically defined by deposition of wild-type tau in the brain. To test this hypothesis, we assayed transposable element transcript levels by NanoString in *Drosophila* expressing human wild-type tau (Supplementary Fig. 2a), which induces neuronal death in *Drosophila*[11], albeit to a lesser extent than $tau^{R406W}$. Multiple previous studies report that expression of human wild-type or R406W mutant tau involve the same major mechanisms of tau-induced neurotoxicity in *Drosophila* models[10,16,20]. Pan-neuronal expression of $tau^{WT}$ significantly increases 10 of 25, and decreases 8 of 22 probes recognizing transposable elements that were identified as increased or decreased, respectively, in $tau^{R406W}$ *Drosophila* based on RNA-seq (Supplementary Fig. 2b, c), suggesting that aberrant transposable element expression is relevant to the greater family of sporadic tauopathies that involve only wild-type tau.

## Loss of transposable element silencing mediates tau-induced neurotoxicity in *Drosophila*.

RNA-seq and NanoString analyses clearly demonstrate that pathogenic tau disrupts baseline levels of transposable element transcripts in the brain. Transposable element activation is classically considered a deleterious event, as mobilization can cause genomic instability[21]. It is now understood, however, that transposable element RNAs have regulatory roles within the cell[1]. In addition, active transposable element mobilization during neurogenesis is thought to positively contribute to somatic diversification[22]. To establish if dysregulation of transposable element expression in the adult brain is beneficial, detrimental, or neutral in the context of tauopathy we determined if genetic manipulation of *flamenco*, a locus in *Drosophila* that is known to restrict transposable element mobilization, mediates $tau^{R406W}$-induced neurotoxicity. Homozygous "permissive" loss of function alleles of *flamenco* allow transposable element mobilization and increase transposable element copy number within the *Drosophila* genome[23,24]. Two different heterozygous loss of function alleles of *flamenco*[23,24] do not induce neuronal death or locomotor deficits in controls, but significantly enhance neuronal death in $tau^{R406W}$ transgenic *Drosophila* (Fig. 2a) and exacerbate tau-induced locomotor deficits (Fig. 2b). Importantly, *flamenco* mutations do not affect total protein levels of transgenic tau (Supplementary Fig. 3a).

Ectopic expression of proteins associated with aberrant activation of the cell cycle in post-mitotic neurons is a well-described feature of human tauopathy[25]. Studies in *Drosophila* indicate that cell cycle activation is causal for neuronal death in tauopathy, and that activation of the cell cycle in neurons is sufficient to induce neuronal death[18]. We find that

heterozygous loss of *flamenco* function exacerbates tau-induced activation of the cell cycle in neurons based on staining with an antibody recognizing proliferating cell nuclear antigen (PCNA) (Fig. 2c). Taken together, these data suggest that loss of transposable element silencing in tau transgenic *Drosophila* is causally linked to neuronal death and promotes neuronal death through aberrant activation of the cell cycle in post-mitotic neurons.

The *flamenco* locus harbors piRNAs that specifically degrade *gypsy, Idefix*, and *ZAM* transposable element transcripts[24], among others. To determine if *flamenco* mutation affects the specific panel of transposable elements that are aberrantly expressed in $tau^{R406W}$ transgenic *Drosophila*, we performed NanoString analyses on *flamenco* loss of function mutants (Supplementary Fig. 3). Rather than a general effect on the panel of transposable elements that are dysregulated by pathogenic tau, these analyses suggest that enhancement of tau-induced neurotoxicity by *flamenco* loss of function is due to activation of specific elements affected by pathogenic tau, and/or additional elements outside of our NanoString codeset.

## Piwi/piRNA depletion is a mechanistic driver of transposable element transcription in tauopathy

Since *flamenco* is known to encode a major piRNA cluster[3,26], and piRNAs have recently been reported to be differentially expressed in the human Alzheimer's disease brain[27,28], we next determined if piRNAs are involved in dysfunctional transposable element control in the tauopathy brain. Small RNA sequencing revealed a significant decrease in 46 of 50 differentially expressed piRNAs in heads of tau transgenic *Drosophila* at day 10 of adulthood (Fig. 3a, Supplementary Table 5, 6). In addition, protein levels of piwi, a central regulator of piRNA biogenesis, are depleted in brains of tau transgenic *Drosophila* based on both immunofluorescence (Fig. 3b) and western blotting (Fig. 3c).

While the function of piwi in regard to piRNA production and transposable element silencing is well established in the germline[29], and piRNAs are known to exist in the *Drosophila* and mammalian brain[30,31], it is currently unknown if piwi reduction affects transposable element transcripts in the brain. To directly quantify the effects of piwi reduction on the panel of transposable elements that are differentially expressed in $tau^{R406W}$ transgenic *Drosophila*, we utilized our custom NanoString codeset to assay transposable element transcript levels in response to pan-neuronal RNAi-mediated piwi knockdown in the absence of transgenic tau. These data indicate that pan-neuronal piwi knockdown (Supplementary Fig. 4a) is sufficient to elevate transcript levels of most of the transposable elements that are increased in $tau^{R406W}$ transgenic *Drosophila* (Fig. 3d), suggesting that tau-induced reduction of piwi and piRNAs is a major contributor to the transposable element expression profile in brains of tau transgenic *Drosophila*.

We next determined if piwi depletion is a causal mediator of neuronal death in tauopathy. RNAi-mediated piwi knockdown using two different non-overlapping RNAi lines is semi-lethal in the context of transgenic tau expression. In the absence of tau, piwi knockdown is sufficient to induce neuronal death by day 10 of adulthood (Fig. 3e). Based on PCNA staining, pan-neuronal piwi reduction is also sufficient to activate the cell cycle in neurons

(Supplementary Fig. 4b), suggesting that pathogenic tau acts through piwi reduction to mediate aberrant cell cycle activation and consequent neuronal death.

We next determined if pan-neuronal overexpression of piwi[32] reduces aberrant transposable element expression and neuronal death in brains of tau transgenic *Drosophila*. Compared to tau expressed alone, piwi overexpression significantly reduces transposable element transcripts that are elevated in tau transgenic *Drosophila* (Fig. 3f). In further support of piwi reduction as a causal contributor to tau-induced neurotoxicity, pan-neuronal piwi overexpression significantly reduces neuronal death in tau transgenic *Drosophila* (Fig. 3g) without affecting total levels of transgenic tau protein (Supplementary Fig. 4c). These data suggest that tau-induced piwi reduction depletes piRNAs, which significantly increases transposable element transcripts and causally contributes to tau-induced neurotoxicity.

## Decondensation of heterochromatin contributes to aberrant transposable element transcription in the adult *Drosophila* brain

We have previously reported widespread relaxation of constitutive heterochromatin, a form of hyper-condensed DNA, in postmortem brains from patients with Alzheimer's disease, which is the most common tauopathy, and in *Drosophila* and mouse models of tauopathy[10]. Tau-induced heterochromatin relaxation plays a causal role in mediating neurodegeneration, as loss of function mutations in *Su(var)205*[33] and *Su(var)3-9*[34], genes encoding heterochromatin protein 1 (HP1) and a histone 3, lysine 9 methyltransferase, respectively, further deplete constitutive heterochromatin in tau transgenic *Drosophila* and enhance tau-induced neuronal death[10].

Based on previous studies that identified constitutive heterochromatin as a silencing mechanism for transposable elements[35], we next determined if genetically promoting heterochromatin relaxation affects the transposable elements that are differentially expressed in tau transgenic *Drosophila.* NanoString analyses reveal that genetically promoting heterochromatin relaxation by loss of function mutations in *Su(var)205* or *Su(var)3-9* causes an increase in most of the transposable element transcripts that were identified as significantly increased in tau transgenic *Drosophila* based on RNA-seq (Supplementary Fig. 5a, b). In the context of our previous report identifying tau-induced heterochromatin decondensation as a central mediator of neurotoxicity in tauopathy, these data suggest that tau-induced heterochromatin decondensation contributes to transposable element dysregulation in brains of tau transgenic *Drosophila*.

## Active transposable element mobilization in neurons of tau transgenic *Drosophila*

56% of the transposable element transcripts that are significantly increased in tau transgenic *Drosophila* are full-length Class I retrotransposons that are fully capable of mobilization. As transcription of DNA to RNA is the first step in retrotransposon mobilization, we next determined if transposable elements actively mobilize in the context of tauopathy. Specifically, we utilized the "gypsy-TRAP" reporter, a GFP-based reporter of *copia* and/or *gypsy* insertion into the *ovo* locus that was developed to detect transposable element mobilization[4]. Because the gypsy-TRAP reporter utilizes the GAL4-*UAS* system that we normally use to express transgenic tau pan-neuronally, we instead utilized an existing

tauopathy model that relies on direct fusion of the human tau transgene to *GMR*, a retinal neuron driver. These flies harbor the V337M-disease-associated[12] form of human mutant tau.

Neuronal death in *Drosophila* models of tauopathy is age-dependent. Accordingly, we do not detect transposable element mobilization in tau$^{V337M}$ transgenic *Drosophila* based on either gypsy-TRAP GFP reporter fluorescence or immunoblotting at day one of adulthood, but detect a significant increase of transposable element mobilization in tau transgenic *Drosophila* based on both GFP fluorescence and immunoblotting at day ten of adulthood. The significant increase in transposable element mobilization in tauopathy compared to controls is sustained in 40-day-old adults (Fig. 4a, b).

## Dietary restriction and inhibition of reverse transcriptase protect against tau-induced transposable element dysregulation and suppress neurotoxicity in tau transgenic *Drosophila*

Dietary restriction extends lifespan in invertebrate and vertebrate systems[36], and reduces age-related transposable element mobilization events in the *Drosophila* fat body[5]. Using the gypsy-TRAP GFP-based reporter of transposable element mobilization[4], we find that 66% dietary restriction reduces tau-induced transposable element mobilization in adult *Drosophila* neurons (Fig. 5a, b). Based on NanoString, dietary restriction significantly reduces the *copia* family at the transcript level, as well as several other transposable elements that are significantly increased in tau transgenic *Drosophila* (Supplementary Fig. 6). TUNEL reveals that dietary restriction suppresses tau-induced neuronal death (Fig. 5c).

Having established that tau-induced transposable element dysregulation is amenable to suppression, we took a pharmacological approach to reduce transposable element mobilization in tauopathy. Like retroviruses, retrotransposons encode machinery, including a capsid protein, polymerase, integrase, and reverse transcriptase, needed to copy themselves and insert the new copy into the genome[37]. 3TC (Lamivudine) is a water-soluble nucleoside analog inhibitor of reverse transcriptase[38] that is FDA-approved for treatment of HIV/AIDS and Hepatitis B, both of which are caused by retroviruses. Like dietary restriction, 3TC is reported to reduce age-associated transposable element mobilization in the *Drosophila* fat body[5]. Tau transgenic flies treated with 10 mM 3TC have significantly reduced gypsy-TRAP reporter activation in the brain (Fig. 6a, b). In addition, 3TC treatment significantly reduces tau-induced neuronal death (Fig. 6c), and significantly alleviates tau-induced locomotor deficits (Fig. 6d) in a dose-dependent manner (Supplementary Fig. 7a, b). Taken together, these data provide additional evidence that transposable element dysregulation is causal for the disease process in tauopathy and is responsive to environmental and pharmacological inhibition.

## Aberrant transposable element transcription in human tauopathy

We next analyzed transposable element expression in human tauopathy using RNA-seq data from cortex (Fig. 7a, b) and cerebellum (Supplementary Fig. 8a, b) of postmortem human control, Alzheimer's disease, and progressive supranuclear palsy patients (Supplementary Table 7). Similar to tau transgenic *Drosophila*, we found that specific subgroups of

transposable elements are upregulated in human tauopathy, while other subgroups are downregulated. Among transposable elements that are upregulated in cortex and cerebellum of both tauopathies, we found a significant over-representation of endogenous retroviruses, while non-LTR retrotransposons are significantly over-represented among transposable elements that are downregulated in cortex and cerebellum of both tauopathies (Fig. 7c, Supplementary Fig. 8c).

We hypothesized that transposable element expression profiles of Alzheimer's disease and progressive supranuclear palsy more closely resemble each other than controls. Principal component analysis supports this hypothesis; in particular, control samples have significantly lower values in the second principal component compared to Alzheimer's disease and progressive supranuclear palsy in both cortex (Fig. 7d) and cerebellum (Supplementary Fig. 8d). We computed the median of the first two principal components over all tauopathy samples and found that the distance of control samples to the median center is significantly further compared to tauopathy samples in both cortex (Fig. 7e) and cerebellum (Supplementary Fig. 8e). Taken together, analyses of human transposable elements clearly reveal a significant transcriptional increase in endogenous retroviruses, and a significant decrease in non-LTR retroelements in postmortem human brain of both Alzheimer's disease and progressive supranuclear palsy patients. In addition, these data suggest that transposable element dysregulation in human tauopathy is a regulated rather than stochastic process, consistent with our studies in tau transgenic *Drosophila*.

## DISCUSSION

We have uncovered a novel, therapeutically targetable mechanism whereby pathogenic tau drives neuronal death (Supplementary Fig. 9, graphical summary). Specifically, our studies identify dysregulation of transposable elements as a consequence of pathogenic tau, and a driver of aberrant cell cycle activation in neurons and subsequent neuronal death. We identify genetic, dietary and pharmacological approaches to reduce transposable element dysregulation and suppress tau-induced neurotoxicity in *Drosophila.* We apply an unbiased transcriptomic approach to extend our findings to postmortem human brains and identify differentially expressed transposable elements in Alzheimer's disease and progressive supranuclear palsy.

Because the complexity and repetitive nature of transposable elements presents challenges to RNA-seq analysis and is associated with a greater frequency of false positives and negatives compared to analysis of canonical messenger RNAs, we performed secondary validation of differentially expressed transposable element transcripts in tau transgenic *Drosophila* by NanoString. While NanoString data show a similar expression trend of most of the transposable elements that are identified as differentially expressed in tau transgenic *Drosophila* by RNA-seq, some of the elements are not confirmed as differentially expressed by NanoString. These data reveal the limitations of each assay when analyzing transposable element transcripts and stress the importance of rigorous secondary validation. Since many members of the *copia* family are increased at the transcript level based on both RNA-seq and NanoString analyses, we speculate that gypsy-TRAP reporter activation is a result of *copia* insertion into the *ovo* locus, rather than *gypsy*. Our attempts to sequence de novo *copia*

insertions within the *ovo* locus in homogenates prepared from tau transgenic *Drosophila* heads resulted in a high frequency of mismatches (data not shown), which is likely a result of the stochastic nature of transposable element insertion.

Based on current understanding, cells have two layers of defense against potentially deleterious transposable element activation: 1) Transposable element transcription is limited by heterochromatin-mediated silencing, and 2) Transposable element transcripts are cleared from the cell by piRNA-mediated degradation. We find that both mechanisms of transposable element suppression are compromised in tauopathy. We speculate that tau-induced heterochromatin decondensation facilitates active transcription of transposable elements, and that tau-induced piwi/piRNA reduction allows those transcripts to persist. While our results are consistent with the effects of heterochromatin decondensation and piwi reduction on transposable element expression that have been reported in the *Drosophila* germline[3,39], our studies reveal a previously undocumented role for heterochromatin- and piRNA-mediated transposable element silencing in the brain. Based on studies in the germline reporting a direct interaction between piwi and HP1[40], and a requirement for Rhino, a member of the HP1 subfamily, for piRNA production[41], it is possible that a direct interaction between piwi and HP1 is also required to silence transposable elements in the brain.

Among upregulated transposable elements in human tauopathy, the human endogenous retrovirus (HERV) family, including HERV-K, is significantly over-represented. Elevated HERV-K transcripts are associated with amyotrophic lateral sclerosis (ALS)[8] and many human cancers, including melanoma, breast cancer, germ cell tumors, renal cancer, and ovarian cancer[42]. A causal association between HERV-K and neuronal dysfunction has previously been established, as ectopic expression of HERV-K or the retroviral envelope protein that it encodes decreases synaptic activity and induces progressive motor dysfunction in mice[8]. Anti-retroviral reverse transcriptase inhibitors inhibit HERV-K activation in cultured cells[43], and are currently in clinical trials for the treatment of ALS. Based on the data presented in the current study, reverse transcriptase inhibitors have significant potential as a novel therapeutic strategy for the treatment of neurodegenerative tauopathies, including Alzheimer's disease.

The ability of *flamenco* loss of function mutations to enhance tau-induced neurotoxicity, and the ability of piwi overexpression, dietary restriction and inhibition of reverse transcriptase to reduce transposable element dysregulation and suppress tau-induced neurotoxicity suggest that tau-induced transposable element dysregulation is deleterious to neuronal survival. In addition to the detrimental effects of transposable element jumping, double stranded RNAs produced by transposable element transcripts, including HERVs, can trigger a type I interferon response through the innate immune system[44]. In light of the HERV increase in human tauopathy and the involvement of the innate immune response as a disease-promoting mechanism in Alzheimer's disease[45], it is tempting to speculate that expression of endogenous retroviruses in human tauopathy contributes to neuroinflammation in addition to promoting genomic instability. In future studies, it will be important to investigate a potential effect of transposable element activation on the innate immune response in the context of tauopathy.

# ONLINE METHODS

## *Drosophila* genetics.

*Drosophila* crosses and aging were performed at 25°C with a 12 h light/dark cycle at 60% relative humidity on a standard diet (Bloomington formulation). Full genotypes are listed in Supplementary Table 1. Pan-neuronal expression of transgenes, including RNAi-mediated knockdown, in *Drosophila* was achieved using the GAL4/UAS system[46] with the *elav* promoter driving GAL4 expression. Retinal expression of transgenes in gypsy-TRAP studies was achieved using the retinal *glass multiple reporter* (*GMR*) promotor. *elav-GAL4/+*, *GMR-Tau*$^{V337M}$, *UAS-GFP, flam*$^{KG00476}$, *flam*$^{OR}$, *Su(var)205*$^{5}$, and *Su(var)3-9*$^{2}$, were obtained from the Bloomington Stock Center. *piwi*$^{v101658}$ and *piwi*$^{v22235}$ were obtained from the Vienna *Drosophila* Resource Center[47] (VDRC, www.vdrc.at). *UAS-tau*$^{R406W}$ and *UAS-tau*$^{WT}$ were a gift from Dr. Mel Feany. Gypsy-TRAP was a gift from Dr. Josh Dubnau. *UAS-HA-piwi* was a gift from Dr. Ruth Lehmann. An equal number of males and females were used in all *Drosophila* assays with the exception of gypsy-TRAP and *flamenco* genetic manipulations. Experiments utilizing the gypsy-TRAP reporter or *flamenco* require two genetic elements on the X chromosome, thus all data points are from female flies.

## RNA sequencing and data analyses.

Library preparation and sequencing were performed by the Genome Sequencing Facility at Greehey Children's Cancer Research Institute at the University of Texas Health San Antonio. For standard RNA-seq, three independent biologically independent replicates were sequenced, each consisting of 500 ng of total RNA from six pooled *Drosophila* heads (18 heads total). Extracted RNA was used for library preparation according to the KAPA Stranded RNA-seq Kit with RiboErase (HMR) sample preparation guide. After quantification by Qubit and Bioanalysis, libraries were pooled for cBot amplification and sequenced on the Illumina HiSeq 3000 platform with 100 base pair paired-end sequencing.

For small RNA-seq, four independent biological replicates were sequenced. 500 ng of total RNA from pooled *Drosophila* heads was used for library preparation according to the NEBNext small RNA sample preparation guide. Due to the abundance of the 2S rRNA in *Drosophila*, we included an additional 2S block step using the oligo (5'-TAC AAC CCT CAA CCA TAT GTA GTC CAA GCA/3SpC3/-3') as described[48]. 2S rRNA blocking was performed directly after 3' SR adapter ligation. 1 μM of the 2S rRNA block oligo was added directly to each ligation reaction on ice, and reactions were incubated at 90°C for 30 sec, then 65°C for 5 min. After 5 min, 1 μl of SR RT primer was added and we proceeded as described in the NEBNext protocol. After small RNA-seq libraries were subjected to quantification by Qubit and Bioanalysis, samples were pooled for cBot amplification and sequenced on the Illumina HiSeq 3000 platform with 50 base pair single-read sequencing. After standard and small-RNA sequencing, CASAVA was used for demultiplexing and fastq files were generated for each sample.

For data cleaning, SortMeRNA[49] v2.1 was used to identify and exclude ribosomal RNA reads, and Trimmomatic[50] v0.36 was used to remove Illumina adaptors. FastQC (http://www.bioinformatics.babraham.ac.uk/projects/fastqc/) v0.11.5 was used for a quality check

before and after the above cleaning steps. The quality of bases in the cleaned reads was above 28 (Sanger/Illumina 1.9 encoding). Reads were aligned to the transposon reference FASTA files (FlyBase[51] Release 6.12), and the quantity of each transposable element was calculated using Salmon[52] v0.7.2. On average, 9 million reads were mapped per sample. DESeq2[53] v1.14.1 was used to identify sequences that were differentially expressed in tau transgenic *Drosophila* compared to controls. Ensembl BioMarts[54] was used to assign genomic locations of differentially expressed transcripts (Supplementary Table 2). Pheatmap (https://CRAN.R-project.org/package=pheatmap) v1.0.8 and Pigengene[55] v1.3.4 R[56] packages were used to generate heatmaps. Values in transposable element heatmaps are standardized Transcripts Per Million[57] (TPM). For presentation clarity in Fig. 1, we subtracted the TPM value of each transposable element from its average across all samples, and then divided the difference by the standard deviation of the TPM value of that particular transposable element. Unscaled heatmaps (Supplementary Fig. 1) represent raw TPM.

piRNA small RNA-seq analyses were similar to the above, with some exceptions. As some tRNAs are mis-annotated as piRNAs, piRNAs that were a subsequence of a tRNA (FlyBase[51] Release 6.16) were removed from analysis. Reads were mapped to the remaining piRNA sequences (piRNABank[58]) as the reference. On average, 16 million reads were mapped per sample. piRNAs with low coverage were excluded as follows: If the sum of reads that mapped to a piRNA in all four tau transgenic *Drosophila* samples was less than three, we considered its expression “undetectable” in tau transgenic samples. Similarly, if the sum of reads that mapped to a piRNA in all four control normal samples was less than three, we considered its expression undetectable in controls. If a piRNA had undetectable expression values both tau transgenic and control samples, it was excluded from our analysis. Raw data for small RNA-seq are included in Supplementary Table 5, and genomic locations of differentially expressed piRNAs are included in Supplementary Table 6.

### NanoString.

We worked with bioinformaticians at NanoString Technologies, Inc. to create a custom codeset consisting of 50 probes: 47 transposable elements identified as differentially expressed by RNA-seq, plus three internal control genes (*RpL32*, *CG15117*, *cyp33*). Codeset sequences are included in Supplementary Table 3. 100 ng of total RNA from pooled *Drosophila* heads was used for NanoString nCounter XT Codeset Gene Expression Assays according to the manufacturer’s protocol. Samples were analyzed by the nCounter™ Prep Station, and results were analyzed using the nCounter™ Digital Analyzer.

### Immunofluorescence and histology.

For tau, piwi, and GFP immunofluorescence, *Drosophila* brains were dissected in PBS and fixed in methanol for 20 min. After blocking with 2% milk in 0.3% triton in PBS for 30 min, brains were incubated with primary antibody diluted in blocking solution overnight at 4°C. After washing with 0.3% triton in PBS, brains were incubated with Alexa488- or Alexa555-conjugated secondary antibodies for 2 h at room temperature. Slides were washed again and incubated with DAPI for 2 min to stain nuclei. Brains were visualized by confocal microscopy (Zeiss LSM 780 NLO with Examiner), and ImageJ was used for analysis. All images shown are a single slice. TUNEL staining was performed in 4 μm sections from

formalin-fixed, paraffin embedded *Drosophila* heads. Secondary detection was performed with DAB. TUNEL-positive neurons were counted throughout the entire brain by bright field microscopy. Antibody concentrations and sources are listed in Supplementary Table 8.

### Western blotting.

Frozen *Drosophila* heads were homogenized in 20 μl Laemmli sample buffer, boiled for 10 min, and analyzed by 4-20% SDS-PAGE. After transferring to nitrocellulose membranes, antigen retrieval was performed by microwaving membranes in one liter of PBS for 15 min. Equal loading was assessed by Ponceau S staining. After blocking membranes in PBS plus 0.05% Tween and 2% milk, membranes were incubated with primary antibodies overnight at 4°C. After washing, membranes were incubated with HRP- conjugated secondary antibodies for 2 h at room temperature. Blots were developed with an enhanced chemiluminescent substrate. Antibody concentrations and sources are listed in Supplementary Table 8. Full scans of western blots are provided in Supplementary Figure 10.

### Locomotor activity.

Walking activity was performed as described previously[10].

### Dietary restriction and 3TC treatment.

“Standard” diet consists of 1.5% yeast, 6.6% light corn syrup, 0.9% soy flour, 6.7% yellow cornmeal, 0.5% agar; “Dietary restriction” diet consists of 0.5% yeast, 2.2% light corn syrup, 0.9% soy flour, 6.7% yellow cornmeal, 0.5% agar, (all wt/vol). Flies were collected at day one of adulthood and placed on a standard or restricted diet. Flies were transferred to fresh food every other day until they were 10 days old, at which point they were fixed, frozen, or assessed for locomotor activity.

For drug treatment, flies were collected at two days old and transferred to standard food or food containing 3TC (Fisher, #50731692, 10 mM except in Supplementary Fig. 3), which was dissolved in water. Flies were transferred to fresh food every other day until they were 10 days old, at which point they were fixed, frozen, or assessed for locomotor activity.

### Analysis of human RNA-seq data.

The Mayo RNA-seq Study on Neuropathological Diseases generated whole transcriptome data for cerebellum and temporal cortex samples from 312 North American Caucasian subjects. These subjects were diagnosed with Alzheimer’s disease, progressive supranuclear palsy, pathologic aging or were elderly controls without neurodegenerative disorders[59]. We downloaded the corresponding clinical data (covariates) from the Accelerating Medicines Partnership – Alzheimer’s Disease (AMP-AD) Knowledge Portal[60]. Specifically, we used the synapseClient R package v1.15-0 (http://www.sagebase.org) to download temporal cortex (syn5223705) and cerebellum (syn3817650) clinical data. 12 cortex (syn6126114) and 10 cerebellum (syn6126119) samples were excluded due to low quality[61,62]. In this study, we also excluded 9 cortex and 15 cerebellum samples that had an RNA Integrity Number (RIN)[63] less than 7. After this filtering, 80 Alzheimer’s disease, 82 progressive supranuclear palsy, and 21 control cortex samples were available, as well as 76 Alzheimer’s disease, 78 progressive supranuclear palsy, and 25 control cerebellum samples. Dr. Nilufer

Taner at the Mayo Clinic provided us with unprocessed RNA-seq data. We converted raw bam files to fastq files using the Picard SamToFastq v2.10.10 tool (http://broadinstitute.github.io/picard). We downloaded human transposable elements from the Genetic Information Research Institute (GIRI) RepBase[64] database in fasta format (http://www.girinst.org/repbase/update/browse.php?type=All&format=FASTA&autonomous=on&nonautonomous=on&simple=on&division=Homo+sapiens&letter=A). The file contains 1073 unique sequences including the 549 ancestral repeats that are shared among all mammals. Using the same pipeline that we described for the analysis of *Drosophila* RNA-seq data, we cleaned the fastq files, aligned them to the human transposable element sequences, and performed differential expression analysis.

### Principal component analyses (PCA) of human RNA-seq data.

We used DESeq2 package and a likelihood ratio test to identify 19 transposable elements that have variable expression in any of the three Alzheimer's disease, progressive supranuclear palsy, or control conditions in cortex (Supplementary Table 7). We then oversampled the control samples to balance the number of samples in each condition by repeating each control sample four times. We performed PCA using the 19 differentially expressed transposable elements, and the 80 Alzheimer's disease, 82 progressive supranuclear palsy, and 84 control samples. A scatterplot of the first two principal components showed that Alzheimer's disease and progressive supranuclear palsy samples cluster together (Fig. 7d). We considered the median of this cluster over all Alzheimer's disease and progressive supranuclear palsy samples as the center of the cluster and computed the distance of each sample to the cluster center. A Kolmogorov–Smirnov Test showed that the control samples do not generally belong to this cluster (Fig. 7e, $P<3*10^{-7}$). We used the ggplot2[65] R package v 2.2.1 to generate violin plots. We performed a similar analysis on cerebellum, which showed that 20 transposable elements have variable expression in Alzheimer's disease, progressive supranuclear palsy, or control (Supplementary Fig. 4a, b, c, Supplementary Table 7). We repeated each control cerebellum sample three times, which provided 75 control samples for PCA. Similar to cortex, the 76 Alzheimer's disease and 78 progressive supranuclear palsy samples cluster together in the scatter plot, and control samples do not generally belong to this cluster (Supplementary Fig. 4d, $P<2*10^{-6}$). In particular, the majority of control samples are below the orange diagonal line.

### Over-representation of specific transposable element classes in differential expression analyses.

All of the four transposable elements that are downregulated in Alzheimer's disease cortex are non-LTR retrotransposons. This is significantly more than expected, since only 239 (22%) of the total 1073 human transposable elements are non-LTR (hypergeometric test, $P=0.002$). Similarly, the non-LTR retrotransposon are overrepresented among downregulated transposable elements in progressive supranuclear palsy cortex ($P=5\times10^{-7}$). We used the sumlog function from the metap package v0.8 to combine these two $P$-values by Fisher's method ($P=2\times10^{-8}$). We multiplied the resulting $P$-value by two to adjust for the two tests conducted in cortex and cerebellum. Similarly, we confirmed that the non-LTR

retrotransposon are also overrepresented in the decreased transposable elements in cerebellum (adjusted $P$=0.01). We used similar tests to show that endogenous retroviruses are overrepresented in the upregulated transposable elements in cortex (adjusted $P$=0.004) and cerebellum (adjusted $P$=0.0003).

### Statistical analyses.

Every reported n is the number of biologically independent replicates. Except when noted otherwise, statistical analyses were performed using a one-way ANOVA with Tukey test when comparing among multiple genotypes, and a two tailed, unpaired Student's $t$-test when comparing two genotypes. Data distribution was assumed to be normal but this was not formally tested. For RNA-seq analysis, a two-sided Wald test[66] was used to calculate false discovery rates (FDR-adjusted $P$-value). For NanoString analyses, we used nSolver Analysis Software v3.0. The central tendency presented is the mean in all cases except NanoString data (median), and error bars represent standard error of the mean. A $P$-value less than 0.05 was considered significant unless otherwise specified. Sample sizes are similar to or greater than those reported in previous publications[4,5,10]. Samples were randomized in all *Drosophila* studies. Investigators were blinded to genotype in all immunohistochemistry, immunofluorescence, and locomotor activity assays. Full statistical analyses are provided in Supplementary Table 9. To improve transparency and increase reproducibility, detailed information on experimental design and reagents can be accessed in the Life Sciences Reporting Summary.

## Supplementary Material

Refer to Web version on PubMed Central for supplementary material.

## Acknowledgements.

We thank J. Dubnau (Stony Brook University) for gypsy-TRAP *Drosophila* stocks and R. Lehmann (New York University School of Medicine) for the $piwi^{OE}$ stock. We acknowledge the Texas Advanced Computing Center (TACC) at the University of Texas at Austin for providing high-performance computing resources: http://www.tacc.utexas.edu. This study was supported by the National Institute for Neurological Disorders and Stroke (BF) and the Owens Foundation (BF). The Mayo human RNAseq study data was led by N. Ertekin-Taner (Mayo Clinic) as part of the multi-PI U01 AG046139 (MPIs Golde, Ertekin-Taner, Younkin, Price) using samples from the following source:

- The Mayo Clinic Brain Bank. Data collection was supported through funding by NIA grants P50 AG016574, R01 AG032990, U01 AG046139, R01 AG018023, U01 AG006576, U01 AG006786, R01 AG025711, R01 AG017216, R01 AG003949, NINDS grant R01 NS080820, CurePSP Foundation, and support from Mayo Foundation.

## References

1. Chuong EB , Elde NC & Feschotte C Regulatory activities of transposable elements: from conflicts to benefits. Nature reviews. Genetics 18, 71–86, doi:10.1038/nrg.2016.139 (2017).
2. Slotkin RK & Martienssen R Transposable elements and the epigenetic regulation of the genome. Nature reviews. Genetics 8, 272–285, doi:10.1038/nrg2072 (2007).
3. Brennecke J et al. Discrete small RNA-generating loci as master regulators of transposon activity in Drosophila. Cell 128, 1089–1103, doi:10.1016/j.cell.2007.01.043 (2007). [PubMed: 17346786]
4. Li W et al. Activation of transposable elements during aging and neuronal decline in Drosophila. Nature neuroscience 16, 529–531, doi:10.1038/nn.3368 (2013). [PubMed: 23563579]

5. Wood JG et al. Chromatin-modifying genetic interventions suppress age-associated transposable element activation and extend life span in Drosophila. Proceedings of the National Academy of Sciences of the United States of America 113, 11277–11282, doi:10.1073/pnas.1604621113 (2016). [PubMed: 27621458]
6. Burns KH Transposable elements in cancer. Nature reviews. Cancer 17, 415–424, doi:10.1038/nrc.2017.35 (2017). [PubMed: 28642606]
7. Li W , Jin Y , Prazak L , Hammell M & Dubnau J Transposable elements in TDP-43-mediated neurodegenerative disorders. PloS one 7, e44099, doi:10.1371/journal.pone.0044099 (2012). [PubMed: 22957047]
8. Li W et al. Human endogenous retrovirus-K contributes to motor neuron disease. Science translational medicine 7, 307ra153, doi:10.1126/scitranslmed.aac8201 (2015).
9. Krug L et al. Retrotransposon activation contributes to neurodegeneration in a Drosophila TDP-43 model of ALS. PLoS genetics 13, doi:10.1371/journal.pgen.1006635 (2017).
10. Frost B , Hemberg M , Lewis J & Feany MB Tau promotes neurodegeneration through global chromatin relaxation. Nature neuroscience 17, 357–366, doi:10.1038/nn.3639 (2014). [PubMed: 24464041]
11. Wittmann CW et al. Tauopathy in Drosophila: neurodegeneration without neurofibrillary tangles. Science 293, 711–714, doi:10.1126/science.1062382 (2001). [PubMed: 11408621]
12. Hutton M et al. Association of missense and 5'-splice-site mutations in tau with the inherited dementia FTDP-17. Nature 393, 702–705, doi:10.1038/31508 (1998). [PubMed: 9641683]
13. Steinhilb ML , Dias-Santagata D , Fulga TA , Felch DL & Feany MB Tau phosphorylation sites work in concert to promote neurotoxicity in vivo. Molecular biology of the cell 18, 5060–5068, doi:10.1091/mbc.E07-04-0327 (2007). [PubMed: 17928404]
14. Dias-Santagata D , Fulga TA , Duttaroy A & Feany MB Oxidative stress mediates tau-induced neurodegeneration in Drosophila. The Journal of clinical investigation 117, 236–245, doi:10.1172/JCI28769 (2007). [PubMed: 17173140]
15. Khurana V et al. A neuroprotective role for the DNA damage checkpoint in tauopathy. Aging cell 11, 360–362, doi:10.1111/j.1474-9726.2011.00778.x (2012). [PubMed: 22181010]
16. Frost B , Bardai FH & Feany MB Lamin Dysfunction Mediates Neurodegeneration in Tauopathies. Current biology : CB 26, 129–136, doi:10.1016/j.cub.2015.11.039 (2016). [PubMed: 26725200]
17. Merlo P et al. p53 prevents neurodegeneration by regulating synaptic genes. Proceedings of the National Academy of Sciences of the United States of America 111, 18055–18060, doi:10.1073/pnas.1419083111 (2014). [PubMed: 25453105]
18. Khurana V et al. TOR-mediated cell-cycle activation causes neurodegeneration in a Drosophila tauopathy model. Current biology : CB 16, 230–241, doi:10.1016/j.cub.2005.12.042 (2006). [PubMed: 16461276]
19. Geiss GK et al. Direct multiplexed measurement of gene expression with color-coded probe pairs. Nature biotechnology 26, 317–325, doi:10.1038/nbt1385 (2008).
20. Bardai FH et al. A Conserved Cytoskeletal Signaling Cascade Mediates Neurotoxicity of FTDP-17 Tau Mutations In Vivo. The Journal of neuroscience : the official journal of the Society for Neuroscience 38, 108–119, doi:10.1523/jneurosci.1550-17.2017 (2018). [PubMed: 29138281]
21. Reilly MT , Faulkner GJ , Dubnau J , Ponomarev I & Gage FH The role of transposable elements in health and diseases of the central nervous system. The Journal of neuroscience : the official journal of the Society for Neuroscience 33, 17577–17586, doi:10.1523/jneurosci.3369-13.2013 (2013). [PubMed: 24198348]
22. Muotri AR et al. Somatic mosaicism in neuronal precursor cells mediated by L1 retrotransposition. Nature 435, 903–910, doi:10.1038/nature03663 (2005). [PubMed: 15959507]
23. Pelisson A et al. About the origin of retroviruses and the co-evolution of the gypsy retrovirus with the Drosophila flamenco host gene. Genetica 100, 29–37 (1997). [PubMed: 9440256]
24. Mevel-Ninio M , Pelisson A , Kinder J , Campos AR & Bucheton A The flamenco locus controls the gypsy and ZAM retroviruses and is required for Drosophila oogenesis. Genetics 175, 1615–1624, doi:10.1534/genetics.106.068106 (2007). [PubMed: 17277359]
25. Frost B , Gotz J & Feany MB Connecting the dots between tau dysfunction and neurodegeneration. Trends in cell biology 25, 46–53, doi:10.1016/j.tcb.2014.07.005 (2015). [PubMed: 25172552]

26. Sarot E , Payen-Groschene G , Bucheton A & Pelisson A Evidence for a piwi-dependent RNA silencing of the gypsy endogenous retrovirus by the Drosophila melanogaster flamenco gene. Genetics 166, 1313–1321 (2004). [PubMed: 15082550]
27. Roy J , Sarkar A , Parida S , Ghosh Z & Mallick B Small RNA sequencing revealed dysregulated piRNAs in Alzheimer's disease and their probable role in pathogenesis. Molecular BioSystems 13, 565–576, doi:10.1039/C6MB00699J (2017). [PubMed: 28127595]
28. Qiu W et al. Transcriptome-wide piRNA profiling in human brains of Alzheimer's disease. Neurobiology of aging 57, 170–177, doi:10.1016/j.neurobiolaging.2017.05.020 (2017). [PubMed: 28654860]
29. Siomi MC , Sato K , Pezic D & Aravin AA PIWI-interacting small RNAs: the vanguard of genome defence. Nature reviews. Molecular cell biology 12, 246–258, doi:10.1038/nrm3089 (2011). [PubMed: 21427766]
30. Ghildiyal M et al. Endogenous siRNAs derived from transposons and mRNAs in Drosophila somatic cells. Science 320, 1077–1081, doi:10.1126/science.1157396 (2008). [PubMed: 18403677]
31. Lee EJ et al. Identification of piRNAs in the central nervous system. RNA (New York, N.Y.) 17, 1090–1099, doi:10.1261/rna.2565011 (2011).
32. Zamparini AL et al. Vreteno, a gonad-specific protein, is essential for germline development and primary piRNA biogenesis in Drosophila. Development (Cambridge, England) 138, 4039–4050, doi:10.1242/dev.069187 (2011).
33. Eissenberg JC , Morris GD , Reuter G & Hartnett T The heterochromatin-associated protein HP-1 is an essential protein in Drosophila with dosage-dependent effects on position-effect variegation. Genetics 131, 345–352 (1992). [PubMed: 1644277]
34. Reuter G , Dorn R , Wustmann G , Friede B & Rauh G Third chromosome suppressor of position-effect variegation loci in Drosophila melanogaster. Molecular and General Genetics 202, 481–487 (1986).
35. Fedoroff NV Presidential address. Transposable elements, epigenetics, and genome evolution. Science 338, 758–767 (2012). [PubMed: 23145453]
36. Longo VD et al. Interventions to Slow Aging in Humans: Are We Ready? Aging cell 14, 497–510, doi:10.1111/acel.12338 (2015). [PubMed: 25902704]
37. Sultana T , Zamborlini A , Cristofari G & Lesage P Integration site selection by retroviruses and transposable elements in eukaryotes. Nature reviews. Genetics 18, 292–308, doi:10.1038/nrg.2017.7 (2017).
38. Coates JA et al. (−)-2'-deoxy-3'-thiacytidine is a potent, highly selective inhibitor of human immunodeficiency virus type 1 and type 2 replication in vitro. Antimicrobial agents and chemotherapy 36, 733–739 (1992). [PubMed: 1380229]
39. Andersen PR , Tirian L , Vunjak M & Brennecke J A heterochromatin-dependent transcription machinery drives piRNA expression. Nature 549, 54–59, doi:10.1038/nature23482 (2017). [PubMed: 28847004]
40. Brower-Toland B et al. Drosophila PIWI associates with chromatin and interacts directly with HP1a. Genes & development 21, 2300–2311, doi:10.1101/gad.1564307 (2007). [PubMed: 17875665]
41. Klattenhoff C et al. The Drosophila HP1 homologue Rhino is required for transposon silencing and piRNA production by dual strand clusters. Cell 138, 1137–1149, doi:10.1016/j.cell.2009.07.014 (2009). [PubMed: 19732946]
42. Gonzalez-Cao M et al. Human endogenous retroviruses and cancer. Cancer Biology & Medicine 13, 483–488, doi:10.20892/j.issn.2095-3941.2016.0080 (2016). [PubMed: 28154780]
43. Tyagi R , Li W , Parades D , Bianchet MA & Nath A Inhibition of human endogenous retrovirus-K by antiretroviral drugs. Retrovirology 14, doi:10.1186/s12977-017-0347-4 (2017).
44. Chuong EB , Elde NC & Feschotte C Regulatory evolution of innate immunity through co-option of endogenous retroviruses. Science 351, 1083–1087, doi:10.1126/science.aad5497 (2016). [PubMed: 26941318]
45. Heneka MT , Golenbock DT & Latz E Innate immunity in Alzheimer's disease. Nature immunology 16, 229–236, doi:10.1038/ni.3102 (2015). [PubMed: 25689443]

## METHODS-ONLY REFERENCES


46. Fischer JA , Giniger E , Maniatis T & Ptashne M GAL4 activates transcription in Drosophila. Nature 332, 853–856, doi:10.1038/332853a0 (1988). [PubMed: 3128741]
47. Dietzl G et al. A genome-wide transgenic RNAi library for conditional gene inactivation in Drosophila. Nature 448, 151–156, doi:10.1038/nature05954 (2007). [PubMed: 17625558]
48. Wickersheim ML & Blumenstiel JP Terminator oligo blocking efficiently eliminates rRNA from Drosophila small RNA sequencing libraries. BioTechniques 55, 269–272, doi:10.2144/000114102 (2013). [PubMed: 24215643]
49. Kopylova E , Noe L & Touzet H SortMeRNA: fast and accurate filtering of ribosomal RNAs in metatranscriptomic data. Bioinformatics (Oxford, England) 28, 3211–3217, doi:10.1093/bioinformatics/bts611 (2012).
50. Bolger AM , Lohse M & Usadel B Trimmomatic: a flexible trimmer for Illumina sequence data. Bioinformatics (Oxford, England) 30, 2114–2120, doi:10.1093/bioinformatics/btu170 (2014).
51. Gramates LS et al. FlyBase at 25: looking to the future. Nucleic acids research 45, D663–D671, doi:10.1093/nar/gkw1016 (2017). [PubMed: 27799470]
52. Patro R , Duggal G , Love MI , Irizarry RA & Kingsford C Salmon provides fast and bias-aware quantification of transcript expression. Nature methods 14, 417, doi:10.1038/nmeth.419710.1038/nmeth.4197https://www.nature.com/articles/nmeth.4197#supplementary-informationhttps://www.nature.com/articles/nmeth.4197#supplementary-information (2017). [PubMed: 28263959]
53. Love MI , Huber W & Anders S Moderated estimation of fold change and dispersion for RNA-seq data with DESeq2. Genome biology 15, 550, doi:10.1186/s13059-014-0550-8 (2014). [PubMed: 25516281]
54. Kinsella RJ et al. Ensembl BioMarts: a hub for data retrieval across taxonomic space. Database : the journal of biological databases and curation 2011, bar030, doi:10.1093/database/bar030 (2011). [PubMed: 21785142]
55. Foroushani A et al. Large-scale gene network analysis reveals the significance of extracellular matrix pathway and homeobox genes in acute myeloid leukemia: an introduction to the Pigengene package and its applications. BMC medical genomics 10, 16, doi:10.1186/s12920-017-0253-6 (2017). [PubMed: 28298217]
56. R Development Core Team. R: A language and environment for statistical computing. (2010).
57. Wagner GP , Kin K & Lynch VJ Measurement of mRNA abundance using RNA-seq data: RPKM measure is inconsistent among samples. Theory in Biosciences 131, 281–285, doi:10.1007/s12064-012-0162-3 (2012). [PubMed: 22872506]
58. Sai Lakshmi S & Agrawal S piRNABank: a web resource on classified and clustered Piwi-interacting RNAs. Nucleic acids research 36, D173–177, doi:10.1093/nar/gkm696 (2008). [PubMed: 17881367]
59. Allen M et al. Human whole genome genotype and transcriptome data for Alzheimer's and other neurodegenerative diseases. Scientific data 3, 160089, doi:10.1038/sdata.2016.89 (2016). [PubMed: 27727239]
60. Hodes RJ & Buckholtz N Accelerating Medicines Partnership: Alzheimer's Disease (AMP-AD) Knowledge Portal Aids Alzheimer's Drug Discovery through Open Data Sharing. Expert opinion on therapeutic targets 20, 389–391, doi:10.1517/14728222.2016.1135132 (2016). [PubMed: 26853544]
61. Purcell S et al. PLINK: a tool set for whole-genome association and population-based linkage analyses. American journal of human genetics 81, 559–575, doi:10.1086/519795 (2007). [PubMed: 17701901]
62. Price AL et al. Principal components analysis corrects for stratification in genome-wide association studies. Nature genetics 38, 904–909, doi:10.1038/ng1847 (2006). [PubMed: 16862161]
63. Schroeder A et al. The RIN: an RNA integrity number for assigning integrity values to RNA measurements. BMC molecular biology 7, 3, doi:10.1186/1471-2199-7-3 (2006). [PubMed: 16448564]
64. Bao W , Kojima KK & Kohany O Repbase Update, a database of repetitive elements in eukaryotic genomes. Mobile DNA 6, 11, doi:10.1186/s13100-015-0041-9 (2015). [PubMed: 26045719]

65. Wickham H ggplot2: Elegant Graphics for Data Analysis. (Springer International Publishing, 2016).

66. Wald A Tests of Statistical Hypotheses Concerning Several Parameters When the Number of Observations is Large. Transactions of the American Mathematical Society 54, 426–482, doi: 10.2307/1990256 (1943).

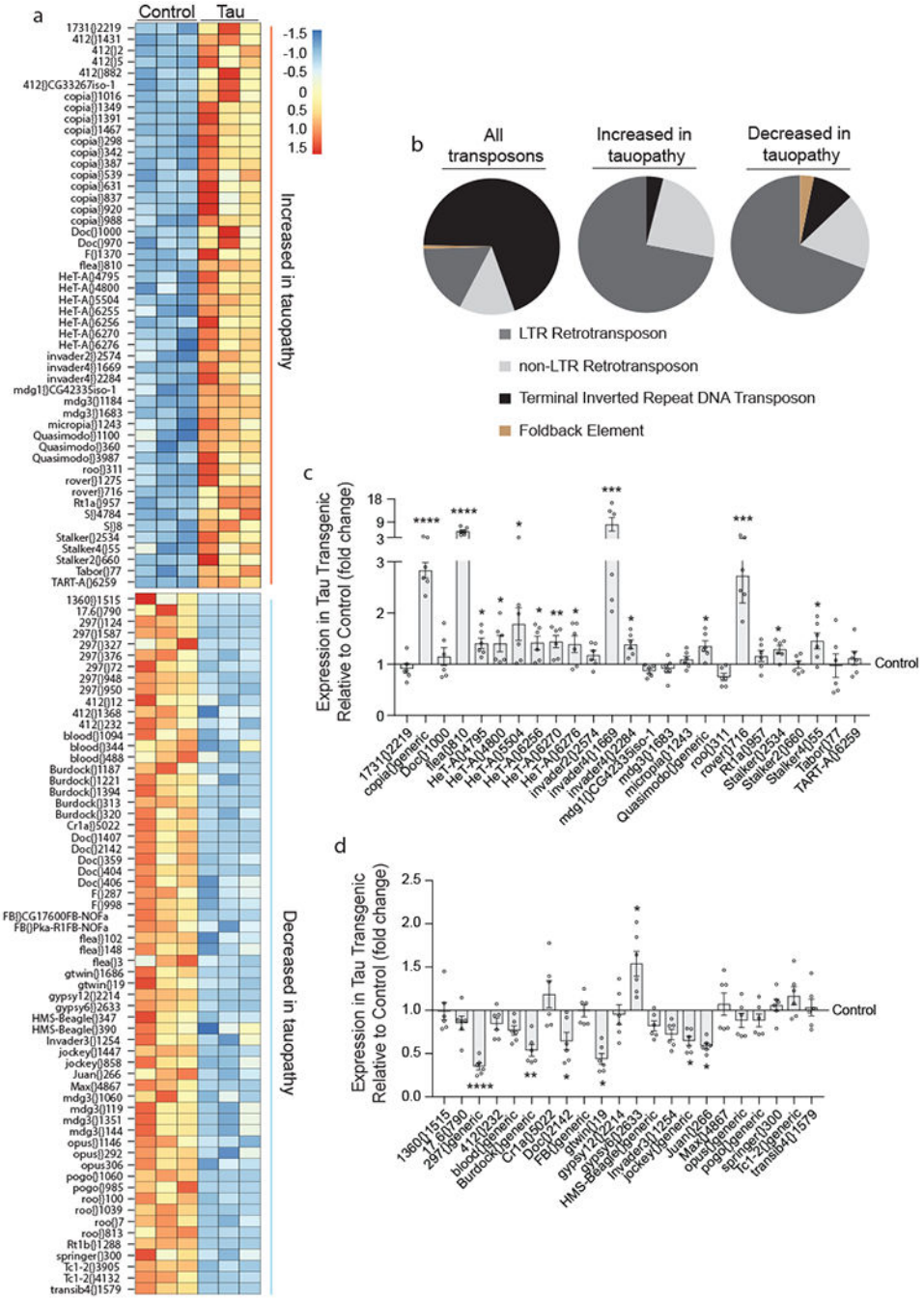


**Figure 1 |. Transposable element transcription in tau$^{R406W}$ transgenic *Drosophila*.**

**a**, Transposable element transcripts that are differentially expressed in tau$^{R406W}$ transgenic *Drosophila* heads versus control based on RNA-seq (two-sided Wald test, FDR, $P$<0.01, n=3 biologically independent replicates, each consisting of RNA pooled from six heads). **b**, Pie charts depicting all classes of transposable elements in *Drosophila*, and classes of transposable elements that are increased or decreased in tau$^{R406W}$ transgenic *Drosophila*. NanoString-based validation of transposable element transcripts that are increased in tauopathy based on RNA-seq (**c**), and transposable elements transcripts that are decreased in

tau$^{R406W}$ transgenic *Drosophila* based on RNA-seq (**d**), n=6 biologically independent replicates each consisting of RNA pooled from 6 heads, values are relative to control, which was set to 1. Unpaired, two-tailed Student's *t*-test, **P*<0.05, ***P*<0.01, ****P*<0.001, *****P*<0.0001. Values are mean ± s.e.m. All flies are 10 days old. Full genotypes are listed in Supplementary Table 1. Transposable elements recognized by "generic" probes are listed in Supplementary Table 4.

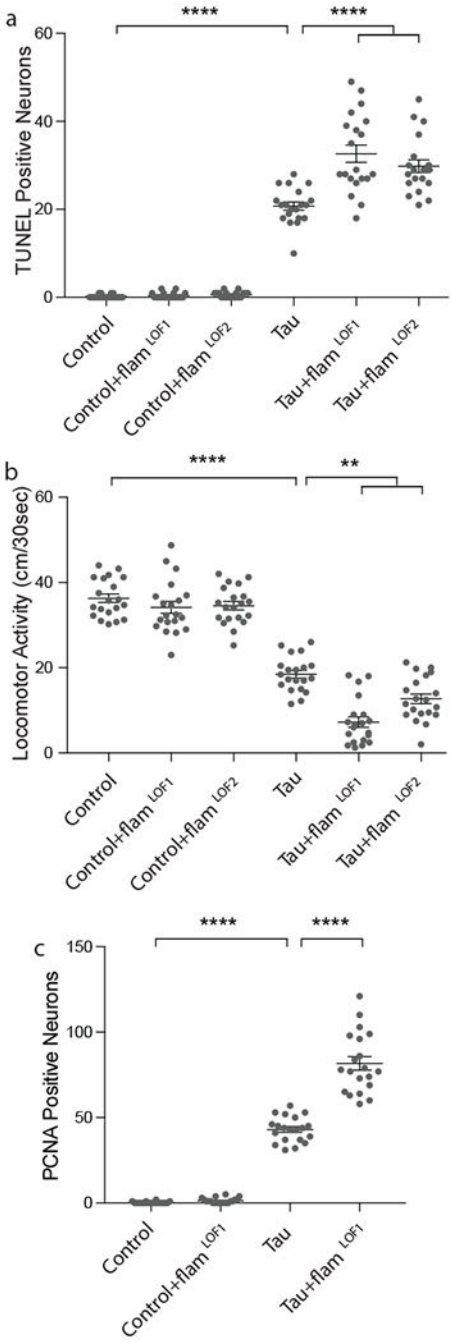


**Figure 2 |. Loss of function mutations in the *flamenco* locus enhance tau$^{R406W}$-induced neurotoxicity.**

Compared to tau$^{R406W}$ expressed alone, tau$^{R406W}$ transgenic *Drosophila* harboring loss of function mutations in the *flamenco* locus have **a**, increased neuronal death, based on TUNEL (one-way ANOVA with Tukey's multiple comparison test) and **b**, reduced locomotor activity (one-way ANOVA with Tukey's multiple comparison test), and **c**, increased activation of the cell cycle based on PCNA staining (one-way ANOVA with Tukey's multiple comparison test). n=20 animals per genotype, per assay. All flies are 10

days old. Values are mean ± s.e.m. n=20 animals per genotype, per assay, ** $P$=0.005, *** $P$<0.001, **** $P$<0.0001. Full genotypes are listed in Supplementary Table 1.

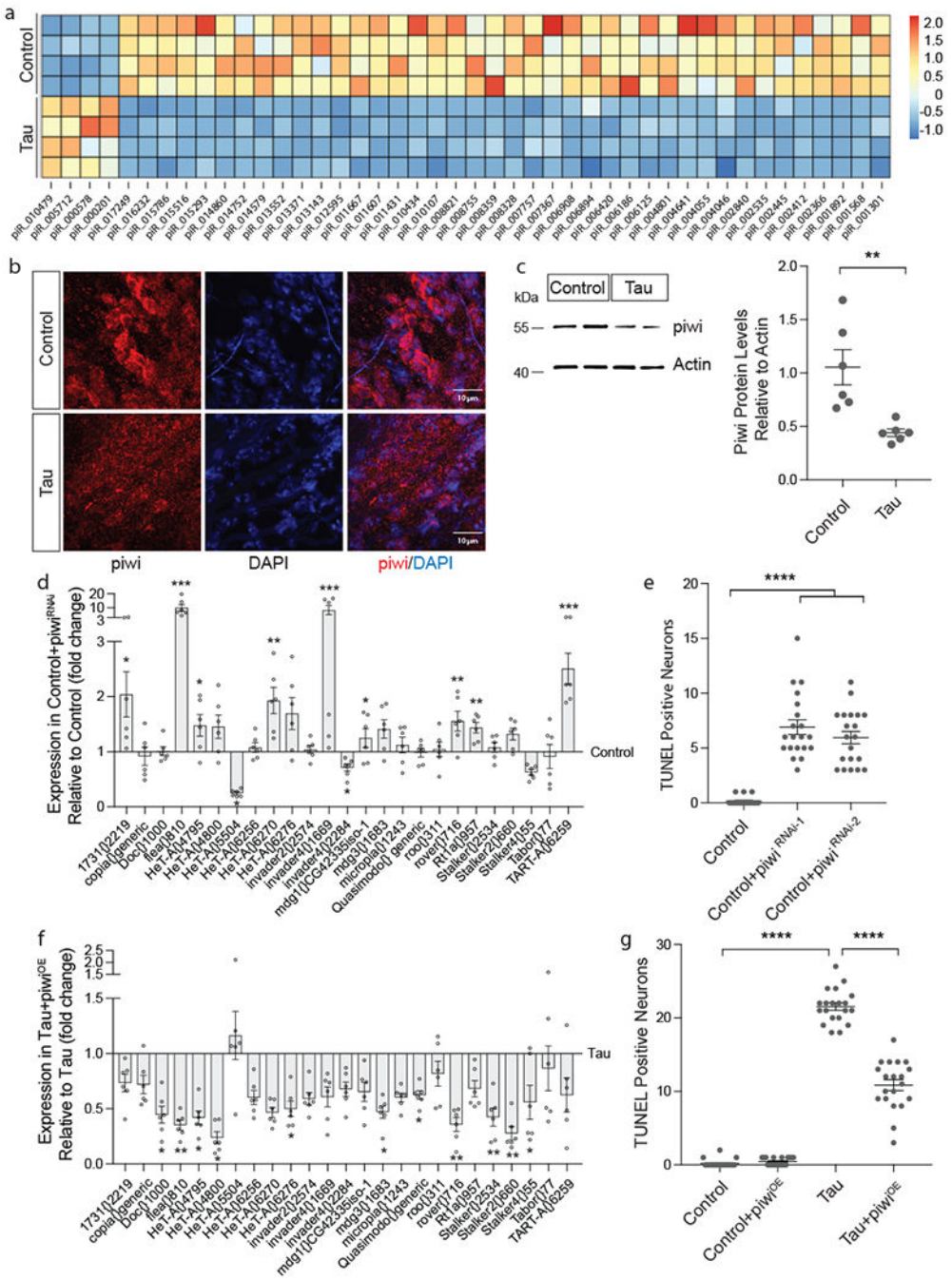


**Figure 3 |. Decreased expression of piwi and piRNAs mediate pathogenic tau$^{R406W}$-induced increase in transposable element transcripts and drive neuronal death.**

**a**, Heatmap reflecting fold change of piRNAs that are differentially expressed in tau$^{R406W}$ transgenic *Drosophila* heads versus controls based on small RNA-seq (two-sided Wald test, FDR, p<0.01, n=4 biologically independent replicates, each consisting of RNA pooled from 6 heads). **b,** Decreased levels of piwi protein (red) in cortex of the tau$^{R406W}$ transgenic *Drosophila* brain based on immunostaining and **c**, western blotting (unpaired, two-tailed Student's *t*-test, ***P*=0.005, n=6 animals per genotype). In **b,** piwi immunostaining was

repeated in 6 animals of each genotype with similar results. Western blot is cropped in **c**, full blot presented in Supplementary Figure 10. **d**, NanoString analysis of transposable element expression in response to RNAi-mediated knockdown of piwi versus control (unpaired, two-tailed Student's *t*-test, **P*<0.05, ***P*<0.01, ****P*<0.001, *****P*<0.0001, n=6 biologically independent replicates each consisting of RNA pooled from 6 heads, values are relative to control, which was set to 1). **e**, Neuronal death assayed by TUNEL in *Drosophila* caused by pan-neuronal RNAi-mediated knockdown of *piwi* (one-way ANOVA with Tukey's multiple comparison test, *****P*<0.0001, n=20 animals per genotype). **f**, NanoString analysis of transposable element expression in response to pan-neuronal piwi overexpression in $tau^{R406W}$ transgenic *Drosophila* versus tau expressed alone (unpaired, two-tailed Student's *t*-test, **P*<0.05, ***P*<0.01, ****P*<0.001, *****P*<0.0001, n=6 biologically independent replicates each consisting of RNA pooled from 6 heads, values are relative to tau expressed alone, which was set to 1). **g**, Neuronal death assayed by TUNEL in $tau^{R406W}$ transgenic *Drosophila* with pan-neuronal piwi overexpression (one-way ANOVA with Tukey's multiple comparison test, *****P*<0.0001, n=20 animals per genotype). All flies are 10 days old. Values are mean ± s.e.m. Full genotypes are listed in Supplementary Table 1. Transposable elements recognized by "generic" probes are listed in Supplementary Table 4.

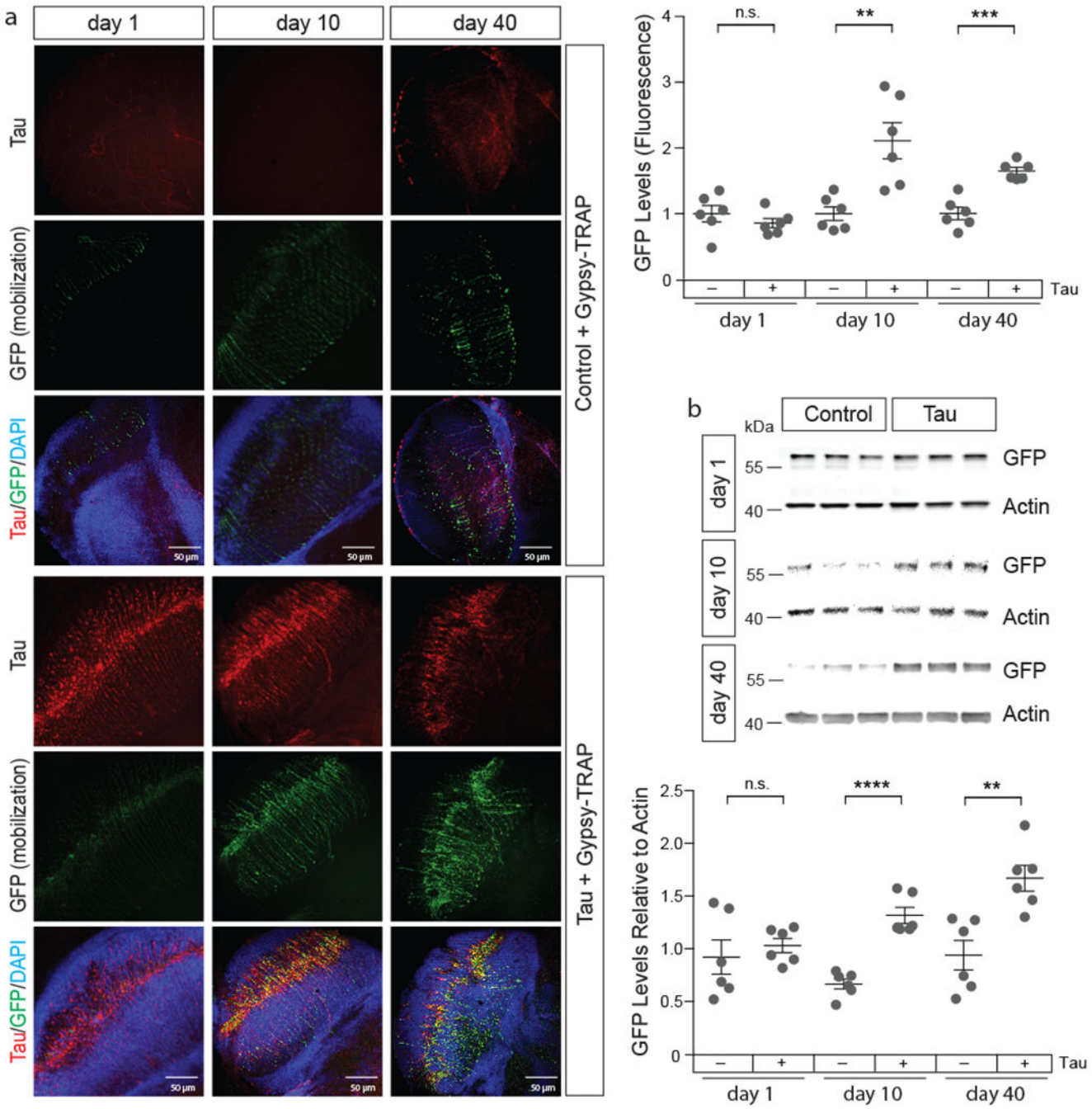


**Figure 4 |. Active mobilization of transposable elements in neurons of tau transgenic *Drosophila*.**

**a**, Gypsy-TRAP (GFP, green), a reporter of transposable element mobilization, is activated in retinal neurons of 10- and 40-day old tau$^{V337M}$ transgenic *Drosophila* compared to control. Brains were stained with the cTau antibody (red) to recognize transgenic tau (unpaired, two-tailed Student's *t*-test, n=6 animals per genotype, per age, n.s.=not significant, ** $P$=0.004, *** $P$=0.0001). **b**, Quantification of gypsy-TRAP activation based on western blotting with an antibody recognizing GFP (unpaired, two-tailed Student's *t*-test, n.s.=not significant, ** $P$=0.003, **** $P$<0.0001). Western blot is cropped, full blot presented

in Supplementary Figure 10. n=6 animals per genotype, per age. Values are mean ± s.e.m. Full genotypes are listed in Supplementary Table 1.

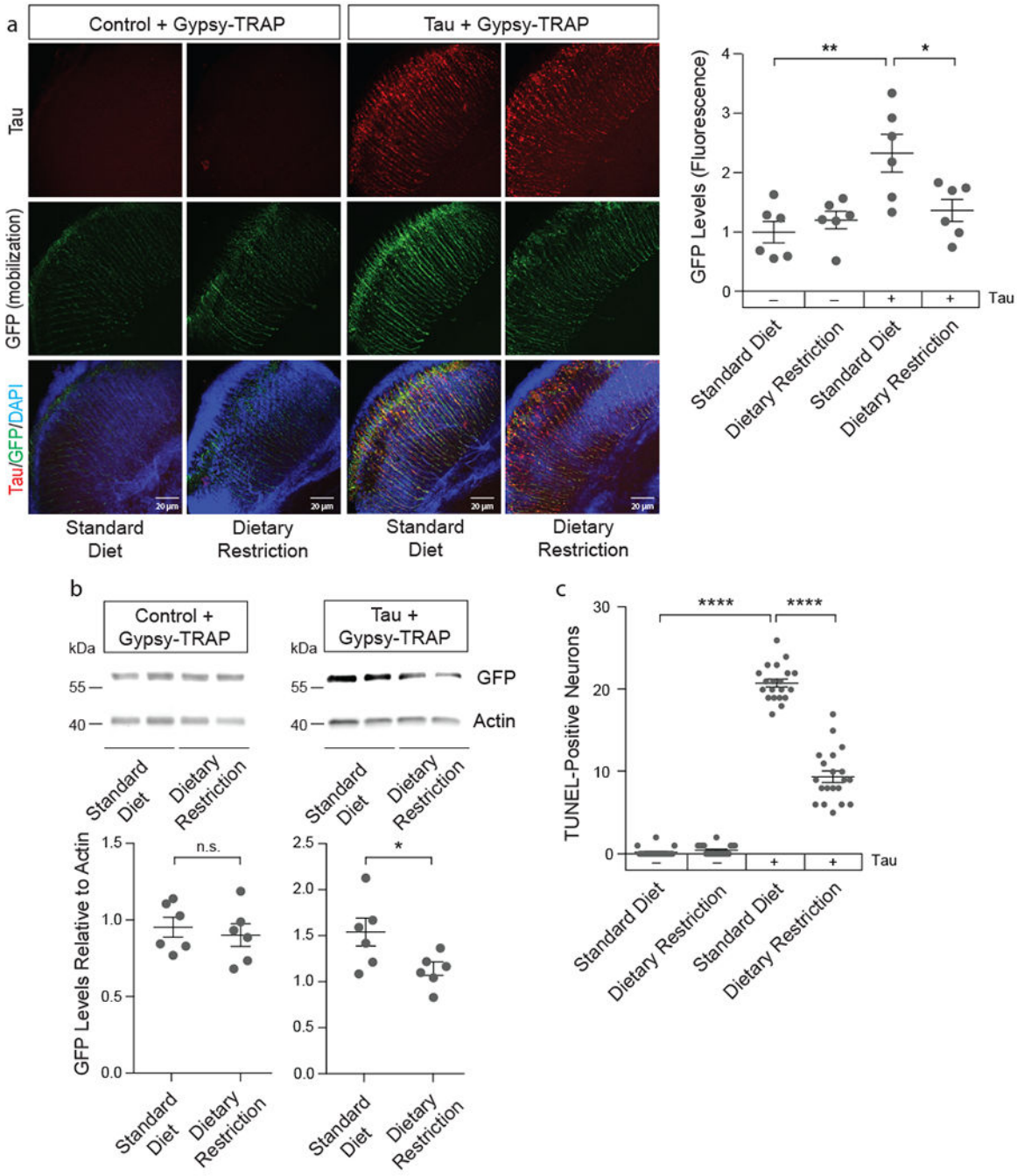


**Figure 5 |. Dietary restriction significantly suppresses tau-induced transposable element mobilization and tau-induced neurotoxicity in *Drosophila*.**

**a**, 66% dietary restriction reduces gypsy-TRAP reporter activation in retinal neurons of tau$^{V337M}$ transgenic *Drosophila* based on GFP fluorescence (one-way ANOVA with Tukey's multiple comparison test, **P*=0.03, ***P*=0.002, n=6 animals per genotype, per treatment) and **b**, western blotting (unpaired, two-tailed Student's *t*-test, n.s.=not significant, **P*=0.04, n=6 animals per genotype, per treatment). Western blot is cropped in **b**, full blot presented in Supplementary Figure 10. **c,** 66% dietary restriction significantly reduces tau$^{R406W}$-induced

neuronal death based on TUNEL (one-way ANOVA with Tukey's multiple comparison test, **** $P$<0.0001, n=20 animals per genotype, per treatment). All flies are 10 days old. Values are mean ± s.e.m. Full genotypes are listed in Supplementary Table 1.

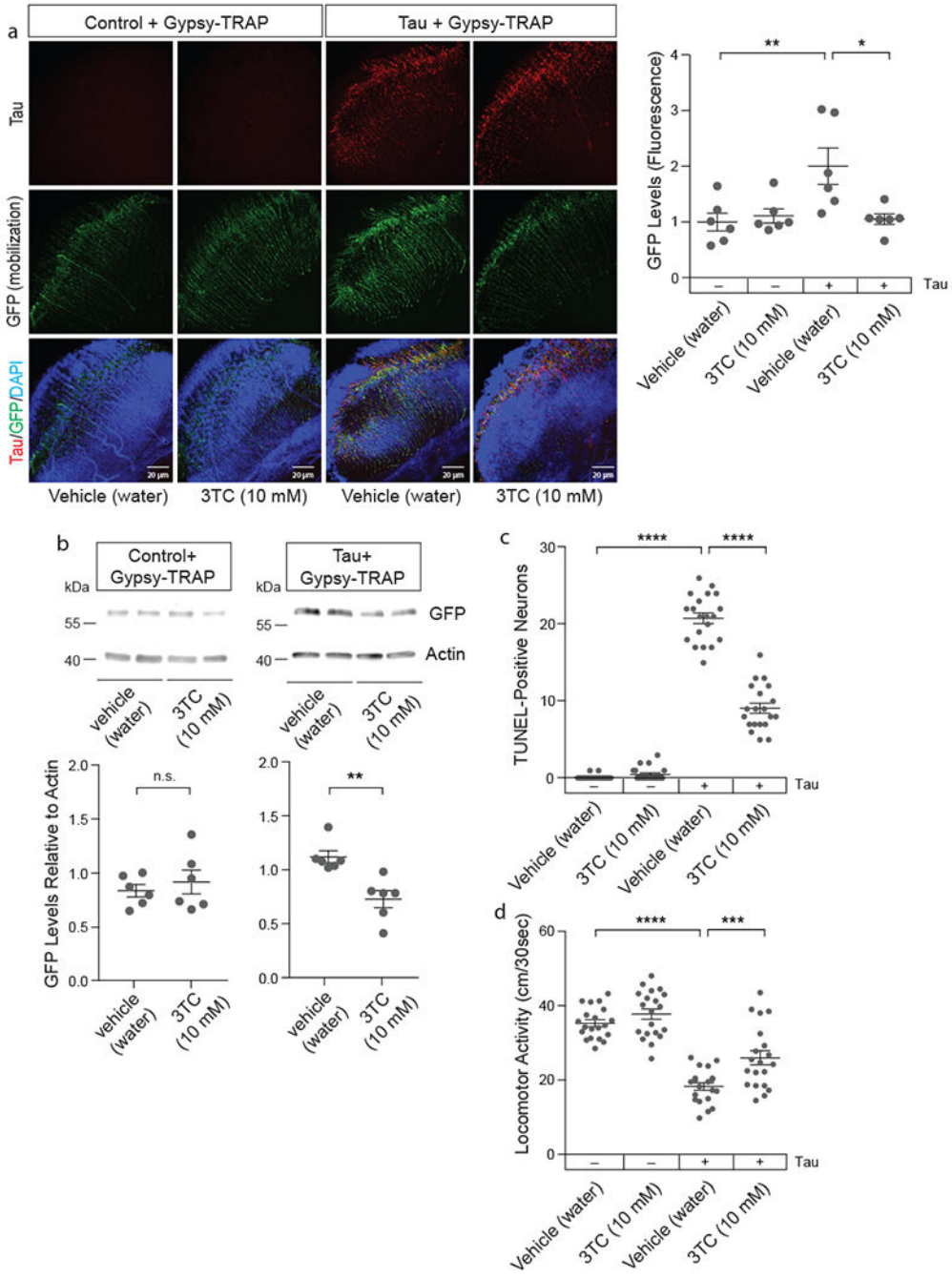


**Figure 6 |. 3TC (Lamivudine), an FDA-approved nucleoside analog reverse transcriptase inhibitor, suppresses tau-induced transposable element mobilization and tau-induced neurotoxicity in *Drosophila*.**

**a**, 10 mM 3TC reduces gypsy-TRAP reporter activation in retinal neurons of tau$^{V337M}$ transgenic *Drosophila* based on GFP fluorescence (one-way ANOVA with Tukey's multiple comparison test, **P*=0.01, ***P*<0.01, n=6 animals per genotype, per treatment) and **b**, western blotting (unpaired, two-tailed Student's *t*-test, n.s.=not significant, ***P*=0.003, n=6 animals per genotype, per drug treatment). Western blot is cropped in **b**, full blot presented in Supplementary Figure 10. **c,** 10 mM 3TC significantly reduces tau$^{R406W}$-induced

neuronal death based on TUNEL (one-way ANOVA with Tukey's multiple comparison test, ****$P$<0.0001, n=20 animals per genotype, per treatment). **d,** 10 mM 3TC significantly alleviates tau$^{R406W}$-induced deficits in locomotor activity (one-way ANOVA with Tukey's multiple comparison test, ***$P$=0.0008, ****$P$<0.0001, n=20 animals per genotype, per treatment). All flies are 10 days old. Values are mean ± s.e.m. Full genotypes are listed in Supplementary Table 1.

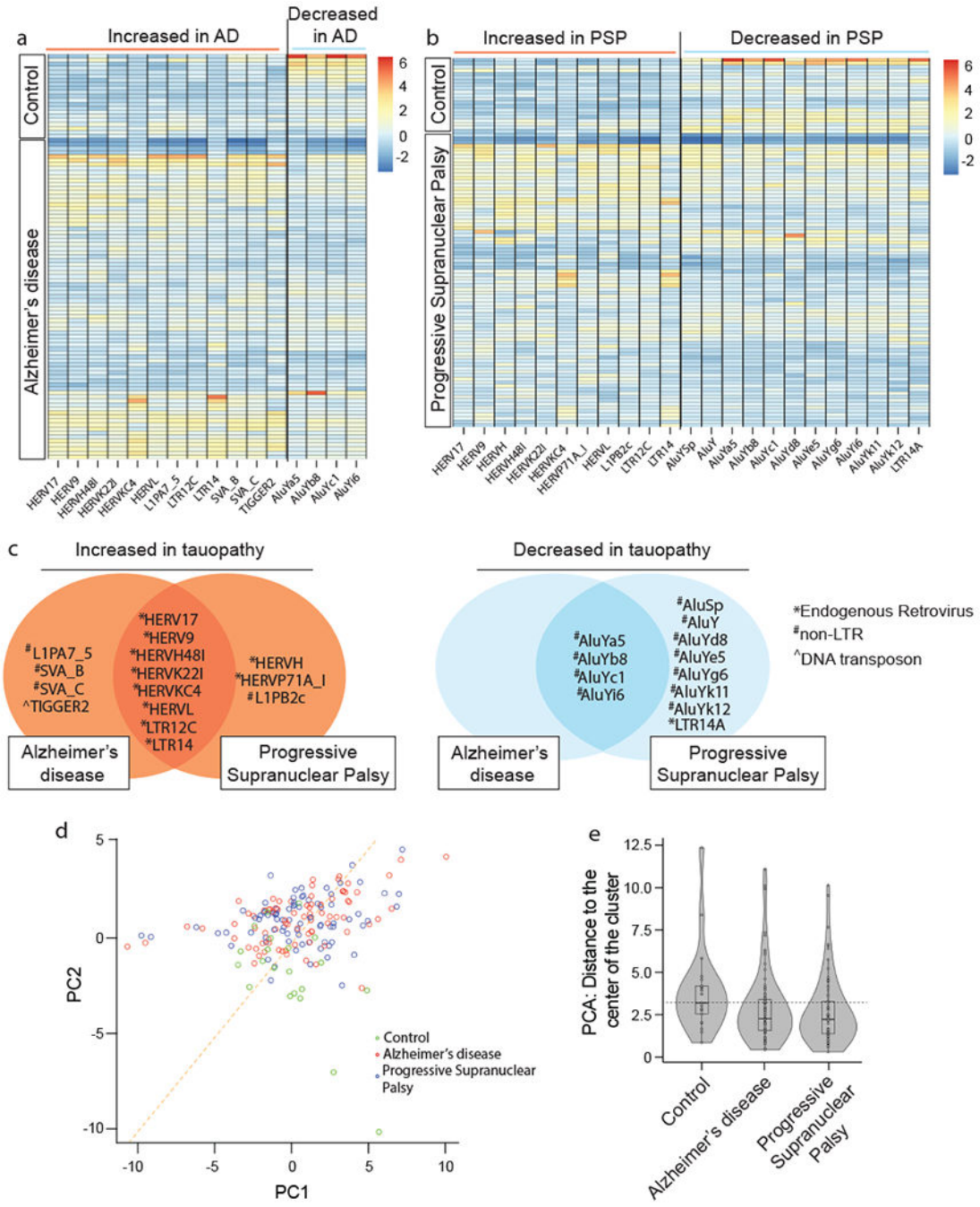


**Figure 7 |. Transposable element expression in cortex of human tauopathy.**

Heatmaps reflecting fold change of differentially expressed transposable elements in human cortex in **a**, control versus Alzheimer's disease (AD), and **b**, control versus progressive supranuclear palsy (PSP), based on RNA-seq. (two-sided Wald test, FDR, $P<0.01$). **c**, Differentially expressed transposable elements in postmortem Alzheimer's disease and progressive supranuclear palsy cortex compared to controls. HERVs are significantly over-represented among transposable element transcripts that are increased in tauopathy (hypergeometric test, adjusted $P=0.004$). Non-LTR are significantly over-represented among

transposable elements that are decreased in tauopathy (hypergeometric test, adjusted $P=4*10^{-8}$). **d**, Principal component analyses of differentially expressed transposable elements in control, Alzheimer's disease, and progressive supranuclear palsy cortex (two-sided Kolmogorov-Smirnov test, $P<10^{-13}$). **e,** Based on principal component analysis of transposable element expression in control versus tauopathy, violin plots show that control samples are relatively farther from the center of the cluster, as defined by the median of Alzheimer's disease and progressive supranuclear palsy samples. Euclidian distance was computed using the first principal components of those transposable elements that are differentially expressed among the three conditions. For control, AD and PSP respectively, minima=0.8, 0.4, 0.3, maxima=12.3, 11.1, 10.1, median=3.2, 2.2, 2.2, mean=3.8, 2.8, 2.6, 1$^{st}$ quantile=2.5, 1.5, 1.3, 3$^{rd}$ quantile=4.2, 3.4, 3.2. Human control n=21, Alzheimer's disease n=80, progressive supranuclear palsy n=82 biologically independent replicates in **a**-**e**.